Near-field infrared nanoscopy of phonon resonant silica and silica-coated gold nanoparticles

Zachary Nuño, Jerry Ochoa, Brandon Hessler, and Yohannes Abate
Department of Physics and Astronomy, California State University Long Beach, CA 90840, USA.
E-Mail: yabate2@csulb.edu, Phone: (562)-985-4912, Fax: (562)-985-7924

ABSTRACT

Single silica capped and uncapped gold nanoparticles are imaged using apertureless near-field optical microscopy (ANSOM) in the infrared frequency range (λ=9-11 μm). While visible frequency imaging can only allow identification of capped and uncapped particles, IR near-field imaging also permits spectroscopic resolved imaging through vibrational resonances. Optical phonon resonances of the silica nanoparticles in pure silica and silica capped Au composite single nanoparticles are imaged in amplitude and phase. The phase spectra show larger contrast near the wavelength where phonon resonant near-field interaction is expected even in capped particles with a thin silica coating layer. Experimental results are in good agreement with dielectric function model calculations which include vertical composition of the nanoparticles in the extended dipole approximation.

Keywords: near-field microscopy, capped particles, silica

1 INTRODUCTION

Coated nanoparticles and core-shell-like nanostructures offer modified physical, electrical and optical properties that are of interest in electronics, photonics, catalysis, nanotechnology and biomedical research.[1] Coated nanoparticles have been used in a wide-range of applications from environmental solutions and green chemistry to biology and medicine. As the ability to synthesize nanoparticles and clusters improves, there is an increasing need to detect and map these materials with chemical and spectroscopic sensitivity. Classical light microscopy allows the resolution of sample features down to about half the illumination wavelength (~250 nm in the visible). This limited resolution hinders single particle characterization and spectroscopic investigation in complex environments. Apertureless near-field scanning optical microscopy (ANSOM) offers ultrahigh optical resolution independently of the wavelength, limited only by the radius of curvature of the probe. The technique also permits spectroscopic resolution through vibrational resonances. ANSOM has been used to detect optical material contrast of single nanoparticles, spectroscopic mapping of single nanobeads and viruses, polydisperse nanoparticles, single carbon nanotubes, diamond, and polymerlike nanoparticles.[2,3] The nanoparticles considered in these studies were pure type, single material particles. Nanoparticle composites, coated nanoparticles or core-shell-like nanostructures remain unexplored by ANSOM. In this work, silica coated gold and pure silica nanoparticles desorbed on silicon substrate are investigated by ANSOM to quantify the wavelength and size dependent near-field resonant phonon polariton interactions in the infrared regime where silica has a vibrational phonon resonance. The experimental manifestation of this resonance is established by calculating in the electrostatic limit the polarizability of an isolated sphere immersed in an electric field.

A dielectric sphere can exhibit a resonance in the infrared due to excitation of infrared surface vibrational modes (surface phonon polaritons).[4] These surface vibrational modes can be resonantly excited in dielectric spheres with a dielectric value Re($\varepsilon/\varepsilon_0$) ~ -2 in the range of the probing infrared laser. Using a simple dielectric function based on the damped harmonic oscillator model that describes the spectra of thin silica films very well,[5] the local field enhancement or resonance of the polarizability function for a silica and silica capped Au spheres are theoretically calculated.[6] Experimentally, the local field enhancement can be imaged in amplitude and phase by a near-field microscope.[4,6,7] In this work, silica and silica capped nanoparticles in the size range between 40-60 nm were used to probe the surface phonon polariton resonance in the region where silica has a vibrational phonon resonance. We demonstrate that the capped particles with a thin shell of silica (<10 nm) can show strong phase contrast and can allow us to distinguish capped particles based on their spectroscopic material signature.

To our knowledge the study reported here is the first near-field spectroscopic study of capped particles that show significant phase contrast in the near-field image. ANSOM allows spectroscopic identification of nanocomposites with nanometer resolution. This remarkable capability of ANSOM should open doors to the investigation of several important problems related to self assembled monolayers, thin oxide layers, photoresist and coatings.

2 EXPERIMENTAL

Simultaneous topography, infrared amplitude and phase contrast imaging is performed using commercial s-NSOM setup (NeaSNOM, neaspec.com) shown in Figure 1 by recording the line-tunable infrared carbon dioxide laser

light scattered from commercial Pt-coated cantilevered Si tips. The vertical oscillation frequency of a tip is 33 kHz with an amplitude of 25 nm. We achieve near-field scattering measurements using a combination of demodulation of the detector signal at higher harmonics of the resonance frequency, $n\Omega$ (demodulation order $n>1$) and a pseudoheterodyne interferometric signal detection scheme for greater background suppression.[8] The pseudoheterodyne detection technique allows simultaneous measurement of near-field optical signal amplitude and phase by interferometric detection of scattered light using a phase-modulated reference wave. This technique has been shown to provide a reliable near-field optical material contrast with a higher background suppression efficiency and ease of implementation compared to other interferometric detection methods.[8]

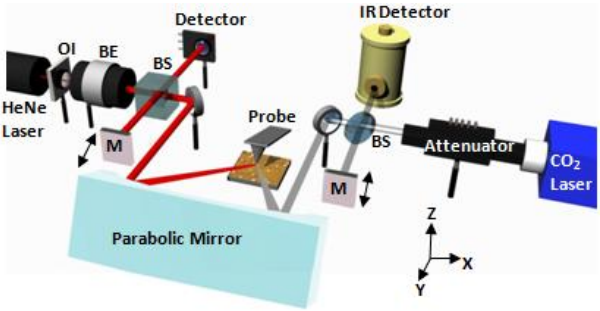

Figure 1. Schematic of the experimental setup (NeaSNOM, neaspec.com), based on a tapping mode atomic force microscope. M = mirror, OI = optical isolator, BE = beam expander, and BS = beam splitter.

Nanoparticle samples were prepared on a Si substrate first cleaned by sonication in methanol and dried with nitrogen gas. The substrate is then dipped in a 0.1% APTMS (s-aminopropyltrimethoxysilane) solution in ethanol, rinsed with pure ethanol and dried with nitrogen gas. Nanoparticle solutions (nanoComposix, nanocomposix.com) were drop-casted on the wafer and allowed to react for 12.5 minutes, then rinsed and dried with ethanol and nitrogen gas respectively. The Samples containing mixed 3 particle kinds (silica, silica capped Au and pure Au nanoparticles) were (Fig. 2) prepared by diluting each solution with an isopropyl alcohol (IPA) solution (3:1 IPA: H_2O) and drop-casting the solutions in the order Au, silica capped gold, then silica particles with 10 minutes reaction time each. Figure 1a,b,d,e are transmission electron-microscopy (TEM) images of monodisperse silica capped Au nanoparticles and pure silica nanoparticles used in these experiments. TEM images shown in figures 2a,b indicates the shapes of the composite silica-Au nanoparticles and the thickness of the capping silica layer (average size of ~10 nm) are highly

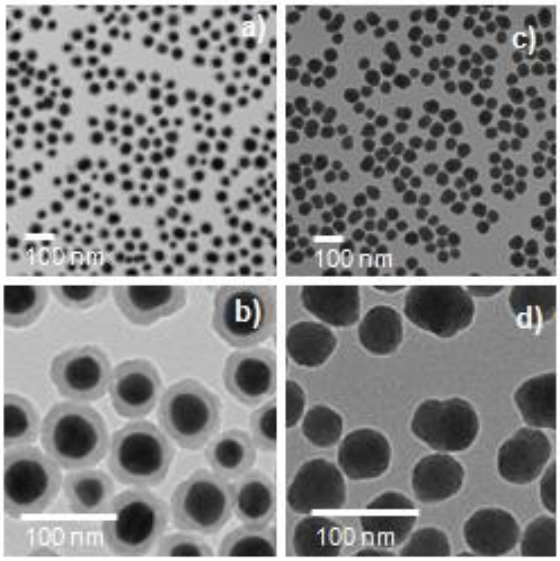

Figure 2. (a) Typical TEM images of monodisperse silica capped Au nanoparticles used in these experiments. (b) A closer view of TEM images of few nanoparticles which shows uniform thickness of the silica capping layer covering Au nanoparticle core. (c) (d) TEM images of pure silica particles.

uniform. Size statistics performed on these samples, pure silica particles and silica capped Au particles, demonstrate size distributions of 10-20%, typical values for many colloidal syntheses.

3 RESULTS AND DISCUSSION

In figure 3 we show topography and optical images in amplitude and phase of pure silica and silica capped Au nanoparticles on a silicon substrate at two of the laser frequencies, ω=1080 cm^{-1} and ω=935 cm^{-1}. For both capped and uncapped particle samples, in the amplitude images, particles appear darker than the substrate and in the phase images they appear brighter than the substrate. At 1080 cm^{-1} where a phonon-polariton resonance is expected (a much stronger phase signal φ_2 (Fig. 3c,f) is observed.[5] The phase contrast is much weaker at off resonance (935 cm^{-1}) as shown in Fig. 3i,l.

To measure the spectral phonon-polariton signature of the silica capped and pure silica particles, amplitude s_2 and phase φ_2 images are taken at 6 different frequencies. Quantitative near-field amplitude and phase measurements were extracted from the raw data, first by averaging over pixel values of the same area of a nanoisland surface to get topographic height values and corresponding near-field amplitude and phase signal values. Careful attention has been given to correlate topographic average values of the same region with the same area average values of amplitude and phase images by correcting the spatial drift between the different images at different

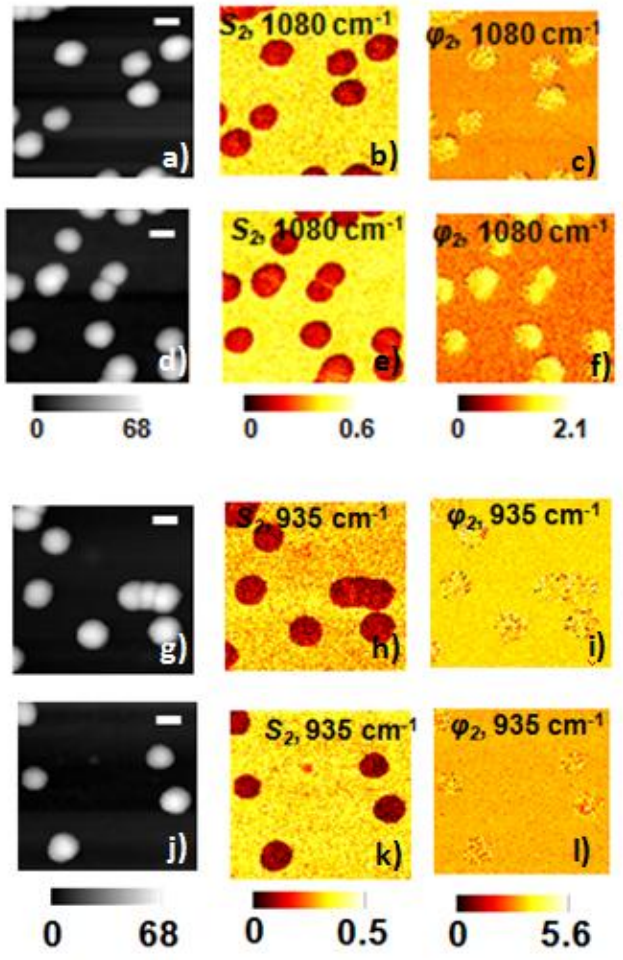

Figure 3. (a) Topography and near-field images of silica capped Au and silica nanoparticles on a silicon substrate. (a)-(c) capped particles at 1080 cm^{-1}, (d)-(f) pure silica particles at 1080 cm^{-1}, (g)-(i) capped particles at 935 cm^{-1}, and (j)-(l) pure silica particles at 935 cm^{-1}. The bars on topography all indicate 100 nm scale.

wavelengths. Signals are then taken on an area on the Si surface and the average amplitude and phase values are calculated for this region at each wavelength. Near-field amplitude values were found by taking the ratio of signal values on the nanoparticles to signal values on the Si surface, and the phase values were calculated in degrees by taking the difference between the signal values on the nanoparticles and Au surface at each wavelength. Several particles with (height~50 nm) were used for analysis resulting in error bars as plotted in Fig. 4a,b. The phase spectra show a phonon-polariton resonance that starts to peak at around 1050 cm^{-1} (Fig. 4b) for both capped and uncapped particles. The amplitude spectra show stronger contrast at higher frequency for the pure particles than that of the capped particles.

To interpret the experimental data, we performed theoretical calculations of the amplitude and phase spectra

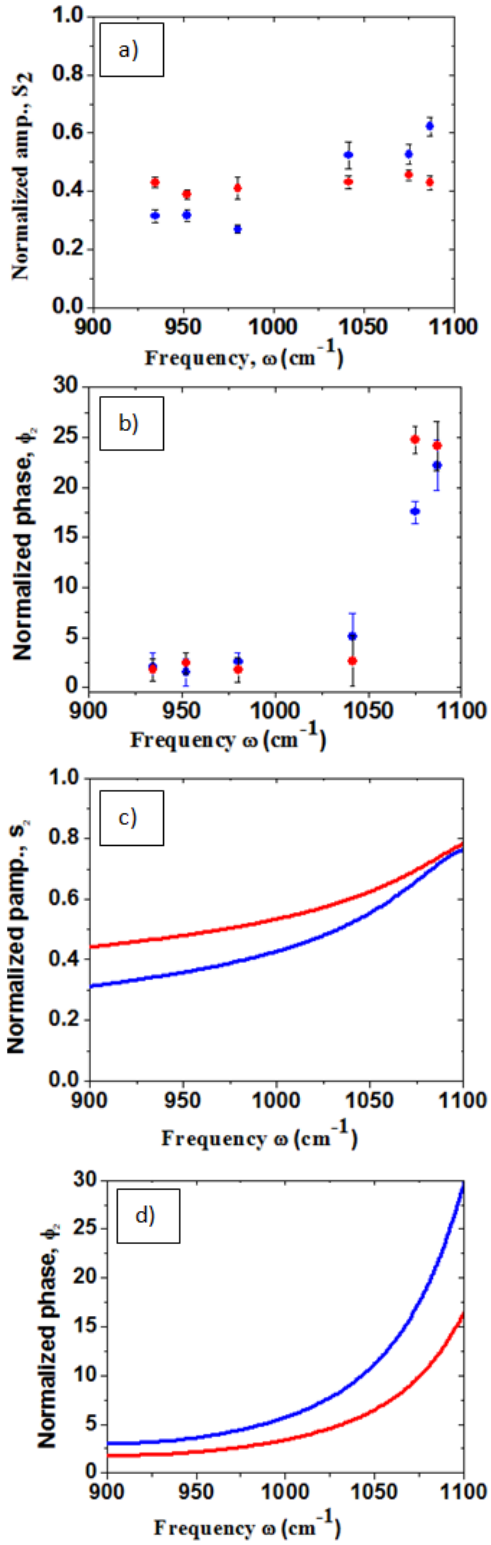

Figure 4. Second harmonic demodulated near-field amplitude s_2 and phase ϕ_2 spectra obtained from ANSOM images of silicon nitride nanoparticles on a silicon substrate. Red points and lines represent results for silica capped Au nanoparticles and blue points and lines represent results for silica nanoparticles, (a) experimental amplitude s_2, with error bars (b) experimental phase ϕ_2 spectra with error bars (c) calculated amplitudes s_2 and (d) calculated phases ϕ_2 spectra.Phase signals are plotted in units of degrees. All values are normalized to that of the Si substrate.

using a dipole–dipole coupling model (see Fig. 4c,d). The model is based on the solution of the electrostatic boundary-value problem (Laplace's equation) for a system of many interacting dipoles in the presence of a substrate.[3,9] In this model, the extended structure of the probing tip is approximated by a point dipole located at the extreme end of the tip (p_t) as shown in figure 3a. The nanoparticles are also considered as point dipoles (p). Both the tip dipole and the nanoparticle dipole interact with their own image dipoles (p'_t and p') generated by the sample surface. The combined polarizability is then described by the sum of the polarizability of the tip dipoles and the nanoparticle dipoles. Since the total polarizability depends on the local dielectric function of the sample, the near-field optical infrared images can thus be considered as dielectric maps of the sample surface where the spatial resolution is given by the size of the tip apex. The dielectric function for pure silica and silica capped Au particles were taken from literature data described by a simple damped harmonic oscillator.[12] The model is further improved by taking into account the tip vibration amplitude (25 nm) and signal harmonic demodulation to simulate experimental conditions. The demodulated 2nd harmonic signal is numerically calculated by Fourier transforming the modulated effective polarizability.

The model calculation results for the second harmonic demodulated near-field amplitudes s_2 and phase φ_2 spectra are shown in figure 4. The calculation reproduces experimental results for both near-field amplitude s_2 and phase φ_2 spectra. Near-field contrast formation in a capped particle must take into account the relative weight the layer and the core metal have in the total interaction. In mid IR frequencies the amplitude contrast between Au and Si substrate is weak compared to, for example visible frequencies. This means that a silica capped particle with an Au core adsorbed on a Si substrate will already result in a weaker contrast in the mid IR frequencies than in the visible regardless of the effect of the capping layer. In addition, in mid IR frequencies, the silica capping layer with a high index contributes significantly to the near-field scattering.[10] As a result of a combined effect of the dielectric values of the Au and the cover layer, the normalized amplitude of a capped particle will be smaller at mid IR as can be seen in Fig. 4a,c. Although the average amplitude signal contrast difference between capped and uncapped particles is in general weak at mid IR, identification of particles in amplitude image is still possible since the normalized $s_2 \sim 0.30$ for pure particles and ~0.40 for capped particles between ω=900-1000 cm^{-1}. On the other hand due to phonon resonance absorption[11] both the pure silica particle and the silica capped-Au result in a higher phase contrast at higher frequency (>1000 cm^{-1}) can be seen in Fig. 4b,d. The narrower and more overlapping amplitude contrast at mid IR frequencies are a result of smaller relative contrast of the capped particles and larger contrast of the pure silica particles.

REFERENCES

1 A. Bao, H. Lai, Y. M. Yang, Z. L. Liu, C. Y. Tao, and H. Yang, Journal of Nanoparticle Research **12** (2), 635-643 (2010); I. Berndt, J. S. Pedersen, and W. Richtering, Angew. Chem.-Int. Edit. **45** (11), 1737-1741 (2006); J. P. Zimmer, S. W. Kim, S. Ohnishi, E. Tanaka, J. V. Frangioni, and M. G. Bawendi, J. Am. Chem. Soc. **128** (8), 2526-2527 (2006); F. Teng, Z. J. Tian, G. X. Xiong, and Z. S. Xu, Catal. Today **93-5**, 651-657 (2004); G. A. Lawrie, B. J. Battersby, and M. Trau, Adv. Funct. Mater. **13** (11), 887-896 (2003); M. Yu, J. Lin, and J. Fang, Chemistry of Materials **17** (7), 1783-1791 (2005); S. K. Basiruddin, A. Saha, N. Pradhan, and N. R. Jana, Journal of Physical Chemistry C **114** (25), 11009-11017 (2010).

2 M. Brehm, T. Taubner, R. Hillenbrand, and F. Keilmann, Nano Lett. **6** (7), 1307-1310 (2006); Y. Abate, A. Schwartzberg, D. Strasser, and S. R. Leone, Chem. Phys. Lett. **474** (1-3), 146-152 (2009); A. Cvitkovic, N. Ocelic, and R. Hillenbrand, Nano Lett. **7** (10), 3177-3181 (2007); A. Hartschuh, E. J. Sanchez, X. S. Xie, and L. Novotny, Phys. Rev. Lett. **90** (9) (2003); Z. H. Kim, S. H. Ahn, B. Liu, and S. R. Leone, Nano Lett. **7** (8), 2258-2262 (2007).

3 A. Cvitkovic, N. Ocelic, J. Aizpurua, R. Guckenberger, and R. Hillenbrand, Phys. Rev. Lett. **97** (6) (2006).

4 R. Hillenbrand, T. Taubner, and F. Keilmann, Nature **418** (6894), 159-162 (2002).

5 R.;Bormann Brendel, D. , J. Appl. Phys. **71**, 1 (1992).

6 A. Huber, N. Ocelic, T. Taubner, and R. Hillenbrand, Nano Lett. **6** (4), 774-778 (2006).

7 R. Hillenbrand, Ultramicroscopy **100** (3-4), 421-427 (2004).

8 N. Ocelic, A. Huber, and R. Hillenbrand, Appl. Phys. Lett. **89** (10) (2006).

9 V. V. Gozhenko, L. G. Grechko, and K. W. Whites, Phys. Rev. B **68** (12) (2003).

10 S. Amarie and F. Keilmann, Phys. Rev. B **83** (4) (2011).

11 J.S. Stiegler, Y. Abate, A. Cvitkovic, Y. Romanyuk, A.J. Huber, S.R. Leone, and R. Hillenbrand, Nano Lett. (2011) *to be submitted.*

12 A.J. Huber, J. Wittborn, and R. Hillenbrand, Nanotechnology 21 (2010) 235702.